CDF Note 10436

Measurement of the Forward Backward Asymmetry in Top Pair Production in the Dilepton Decay Channel using 5.1 fb^{-1}

The CDF Collaboration
URL http://www-cdf.fnal.gov
(Dated: March 10, 2011)

We report on a measurement of the inclusive forward-backward asymmetry in $t\bar{t}$ production in the dilepton channel using 334 dilepton candidates collected in 5.1 fb^{-1} of collected data. The production angle of top is measured using the rapidity difference between top and anti-top quarks ($\Delta \mathrm{y}_{t-\bar{t}}$). The reconstructed asymmetry, without corrections, is $A_{fb}(data) = 0.14 \pm 0.05_{stat}$. The measurement is corrected for backgrounds, detector acceptance, and resolution effects, which serve to bias and/or dilute the measurement. After subtracting the predicted background contribution, the and the asymmetry of the background subtracted $\Delta \mathrm{y}_{t-\bar{t}}$ is found $A_{fb}(bkg - sub) = 0.21 \pm 0.07_{stat} \pm 0.02_{bkg-shape}$. Finally, detector and acceptance effects are corrected by assuming a linear dependence of the production angle on the underlying asymmetry. The fully corrected measured asymmetry is $A_{fb} = 0.42 \pm 0.15_{stat} \pm 0.05_{syst}$, which is to be compared to the standard model prediction, $A_{fb}(theory) = 0.06 \pm 0.01$.

I. INTRODUCTION

We describe a measurement of the $t\bar{t}$ forward backward asymmetry in events where the top decay products are two leptons, two bottom quarks, and large missing transverse energy, often referred to as the dilepton channel. Recent measurements of the forward backward asymmetry at the Tevatron have indicated a larger asymmetry than expected by the standard model [1]. The measurement described in this paper use events uncorrelated to the events used in these previous measurements, which provide an independent test of the larger than expected effect.

There are several possible reasons for a forward backward asymmetry in top production. First and foremost, next-to-leading-order (NLO) QCD predicts a small but non-zero charge asymmetry. Evaluated at leading order, heavy flavor pair production via $q\bar{q}$ or gg does not discriminate between quark and anti-quark. But at next-to-leading order, radiative corrections involving a virtual or real gluon in $q\bar{q} \rightarrow Q\bar{Q}$ lead to a difference in the production of Q and $\bar{Q}$, and consequently a charge asymmetry. The asymmetry originates from interference between charge even and odd diagrams. The overall charge asymmetry is positive and predicted to be about 6% [2]. In this analysis we assume CP symmetry is conserved and therefore, the front-back asymmetry will be equal to the predicted charge asymmetry. Alternatively, new physics can appear which could modify the standard model picture, such as a new massive colored particle with axial vector coupling. Several possible new physics could create a sizable forward backward asymmetry without significantly modifying the rate of top production at energies at the Tevatron, which has been measured to be consistent with standard model predictions [3].

In this note, we present the measurement of A_{fb} in $t\bar{t}$ production in the dilepton decay channel, using 5.1 fb^{-1} of data. We first isolate a sample of top event candidates and predict their background composition. We have developed an algorithm which depends on the topology of top quark events to reconstruct both the top and anti-top direction. The difference between the top and anti-top rapidity is directly proportional to the angle of the top quark with respect to the incoming parton in the top-antitop rest frame. The asymmetry of the top anti-top rapidity difference is therefore equal to the top quark forward backward asymmetry in the top anti-top rest frame. The measured production angle is distorted from its true value by a number of experimental complications. Corrections for these effects are applied to the forward and backward counts to produce a measurement of A_{fb} which can be compared to the theoretical prediction.

II. EVENT SELECTION

Events are collected at the Collider Detector Facility (CDF) at Fermi National Accelerator Laboratory [4, 5]. The components relevant to these cross section measurements include the silicon tracker, the central outer tracker (COT), the electromagnetic and hadronic calorimeters, the muon detectors, and the luminosity counters.

At the Tevatron, the top quark is expected to be produced mostly in pairs through quark anti-quark annihilation and gluon fusion [6]. Assuming unitarity of the three-generation CKM matrix, top quarks decay almost exclusively to a W-boson and a bottom quark. Because of this, the signature of $t\bar{t}$ events in the detector is determined by how the W bosons decay. The analysis presented here identify $t\bar{t}$ events using the decay of both W-bosons to a lepton and a neutrino.

Candidate $t\bar{t}$ events are first collected through central high-p_T lepton triggers [5, 7]. Each event is required to have two high-p_T electrons or muons, or an event with one high-p_T electron and one high-p_T muon. The charge of the leptons must be measured to have opposite sign. Tau-lepton reconstruction has lower purity and therefore taus are not specifically selected, though some events pass selection when a tau decays leptonically. Electrons can be central ($|\eta| < 1.1$) or forward ($1.2 < |\eta| < 2.8$). Each electron is required to have a track in the COT along with a large clustered energy deposit in the electromagnetic calorimeter, $E_T > 20$ GeV, with little energy in the hadronic calorimeter. Muons are required to have a high-p_T track in the COT ($p_T > 20$ GeV and $|\eta| < 1.0$), a small amount of minimum-ionizing energy in the calorimeters, and associated set of hits in the muon detectors. Events are required to have a large amount of missing transverse energy as evidence of the neutrinos from the W-boson decay: $\not\!\!E_T > 25$ GeV [8] or $\not\!\!E_T > 50GeV$ if any lepton or jet is closer than 20° from the direction of $\not\!\!E_T$. At least two reconstructed jets are required, where a jet is identified using a fixed cone algorithm of radius $R = \sqrt{(\Delta\eta)^2 + (\Delta\phi)^2} = 0.4$ [9]. Each jet is required to have transverse energy $E_T > 15$ GeV and $|\eta| < 2.5$. To reduce background, an additional requirement is placed on the scalar sum (H_T) of the transverse energy of the leptons, $\not\!\!E_T$, and jets ($H_T > 200$ GeV). Details of the event selection is discussed in the paper of top production cross section using dilepton events [18], except that additional requirement of $|\delta Z_\ell| < 4cm$ is made to make sure that the two leptons are from the same interaction, where $|\delta Z_\ell|$ is the absolute value of the Z position difference of the two leptons.

There are several physics processes which can mimic a $t\bar{t}$ event in the selected data sample, such as Z/γ^* decays to electrons or muons, diboson production (WW, ZZ, WZ), Z-bosons decaying to two taus, W-boson events associated

TABLE I: Number of expected signal and background events, as predicted by the $t\bar{t}$ production cross section measurement in the dilepton decay channel for 5.1 fb^{-1}

Process	Events
WW	11.7 ± 2.4
WZ	3.5 ± 0.6
ZZ	2.3 ± 1.8
Wγ	0.4 ± 0.4
DY$\rightarrow \tau\tau$	12.3 ± 2.2
DY$\rightarrow ee + \mu\mu$	22.4 ± 3.2
Fakes	34.3 ± 14.7
$t\bar{t}$	237.1 ± 11.3
Total	324.0 ± 28.3
Data	334

with a photon, and events where a jet is falsely identified as a lepton (fake). These processes are modeled by a mixture of event generator simulations and data-based techniques.

Z+jets, and diboson events are generated using ALPGEN, PYTHIA, and MADEVENT respectively, where PYTHIA is used to model parton showering and the underlying event for all generated samples [10–14]. CTEQ6.6 parton distribution functions (PDF) are used in all MC simulations [15]. CDFSIM, a GEANT-based simulation, is used to model the CDF detector response [16, 17].

Events where Z/γ^* decays to leptons and $Z \rightarrow \tau\tau$ events are generated using ALPGEN, and diboson events are generated with PYTHIA. All other processes pass selection by mis-identifying one or more leptons in the detector. These fake lepton events are dominated by W boson events with associated jets. Fakes are modeled by W+jets events where one jet passes selection criteria such that it is a good candidate to fake lepton selection. The predicted number of events for each background process, along with the number of expected $t\bar{t}$ events at the measured cross section, is calculated from the measurement of the $t\bar{t}$ cross section in the dilepton decay channel [18]. The predictions are shown compared to data in Table I. After $t\bar{t}$ candidates are selected, the production angle of the top and anti-top quarks are reconstructed.

III. RECONSTRUCTION

After $t\bar{t}$ candidates are selected, the production angle of the top and anti-top quarks are reconstructed. This is complicated by the fact that un-detectable neutrinos are among the decay products of the top quarks, which leads to six unknown variables from the neutrino momenta ($\vec{p}_\nu$, $\vec{p}_{\bar{\nu}}$).

$$\begin{aligned}
M^2_{\ell^+\nu} &= (|\vec{p}_{\ell^+}| + |\vec{p}_\nu|)^2 - (\vec{p}_{\ell^+} + \vec{p}_\nu)^2 = M^2_W \\
M^2_{\ell^-\bar{\nu}} &= (|\vec{p}_{\ell^-}| + |\vec{p}_{\bar{\nu}}|)^2 - (\vec{p}_{\ell^-} + \vec{p}_{\bar{\nu}})^2 = M^2_W \\
M^2_{\ell^+\nu b} &= (|\vec{p}_{\ell^+}| + |\vec{p}_\nu| + |\vec{p}_b|)^2 - (\vec{p}_{\ell^+} + \vec{p}_\nu + \vec{p}_b)^2 = M^2_t \\
M^2_{\ell^-\bar{\nu}\bar{b}} &= (|\vec{p}_{\ell^-}| + |\vec{p}_{\bar{\nu}}| + |\vec{p}_{\bar{b}}|)^2 - (\vec{p}_{\ell^-} + \vec{p}_{\bar{\nu}} + \vec{p}_{\bar{b}})^2 = M^2_t \\
(\vec{p}_\nu + \vec{p}_{\bar{\nu}})_x &= (\not{E}_T\ )_x \\
(\vec{p}_\nu + \vec{p}_{\bar{\nu}})_y &= (\not{E}_T\ )_y\,.
\end{aligned} \tag{1}$$

With these constraints, there are still up to four possible solutions to the neutrino momenta, as well as two combinations due to the $b - \bar{b}$ ambiguity. Additional constraints are required to choose from these possibilities. For each possible solution, $p_z^{t\bar{t}}$, $p_T^{t\bar{t}}$, and $M_{t\bar{t}}$ are calculated, and compared to the probability distribution functions (PDF) of these variables based on standard model expectations. The most likely solution is chosen from likelihood function based on these PDFs.

$$\mathcal{L}\left(\vec{p}_\nu, \vec{p}_{\bar{\nu}}, E_b, E_{\bar{b}}\right) = P\left(p_z^{t\bar{t}}\right) P\left(p_T^{t\bar{t}}\right) P\left(M_{t\bar{t}}\right) \times \tag{2}$$
$$\frac{1}{\sigma_{\rm jet1}} \exp\left[-\frac{1}{2}\left\{\frac{E_{\rm jet1}^{\rm meas} - E_{\rm jet1}^{\rm guess}}{\sigma_{\rm jet1}}\right\}^2\right] \times \frac{1}{\sigma_{\rm jet2}} \exp\left[-\frac{1}{2}\left\{\frac{E_{\rm jet2}^{\rm meas} - E_{\rm jet2}^{\rm guess}}{\sigma_{\rm jet2}}\right\}^2\right] \times$$
$$\frac{1}{\sigma_x^{\rm MET}} \exp\left[-\frac{1}{2}\left\{\frac{\not{E}_x^{\rm meas} - \not{E}_x^{\rm guess}}{\sigma_x^{\rm MET}}\right\}^2\right] \times \frac{1}{\sigma_y^{\rm MET}} \exp\left[-\frac{1}{2}\left\{\frac{\not{E}_y^{\rm meas} - \not{E}_y^{\rm guess}}{\sigma_y^{\rm MET}}\right\}^2\right],$$

The performance of the algorithm in determining $\Delta y_{t-\bar{t}}$ is shown in Figure 1. The reconstructed difference in rapidity between top and anti-top ($\Delta y_{t-\bar{t}}$) are shown in Figure 2. From this distribution, the uncorrected forward backward asymmetry observed in data is $A_{fb}(data) = 0.14 \pm 0.05_{stat}$.

An alternative view of the production angle is to study the difference in rapidity between the leptons. The decay products of the top quark, on average, follow the initial direction of the momentum of the top quark, especially for top quarks with high momentum. Figure 3 shows the difference in rapidity between the two leptons in the event. The forward backward asymmetry observed in the data is $A_{fb}(data, \eta_\ell) = 0.14 \pm 0.05_{stat}$, which is nearly identical to the asymmetry observed in the reconstructed $\Delta y_{t-\bar{t}}$ distribution.

Figure 4, 5, and 6 show the reconstructed Δy_t distributions for the DIL candidates in the e-e, e-μ, and μ-μ channels, respectively. The raw asymmetries are found to be

$$\begin{aligned} A_{\rm obs}^{ee} &= 0.270 \pm 0.112(\text{stat.}) \qquad (\text{Pred.} : -0.010 \pm 0.070) \\ A_{\rm obs}^{e\mu} &= 0.060 \pm 0.077(\text{stat.}) \qquad (\text{Pred.} : -0.004 \pm 0.037) \\ A_{\rm obs}^{\mu\mu} &= 0.170 \pm 0.102(\text{stat.}) \qquad (\text{Pred.} : -0.039 \pm 0.078)\ . \end{aligned}$$

The results shows all lepton flavor channels have positive asymmetries.

It is found that the forward-backward asymmetry is dependent on $M_{t\bar{t}}$, the invariant mass of the $t\bar{t}$ system. Figure 7 shows the reconstructed $M_{t\bar{t}}$ distribution of dilepton candidates in 5.1 fb^{-1} data. The distribution of data is consistent with the prediction.

Figure 8, 9 show the reconstructed Δy_t distributions for the DIL candidates with the reconstructed $M_{t\bar{t}} < 450$ GeV and $M_{t\bar{t}} > 450$GeV, respectively. The raw asymmetries are found to be

$$\begin{aligned} A_{\rm obs}^{<450\ \rm GeV} &= 0.104 \pm 0.066(\text{stat.}) \qquad (\text{Pred.} :\ 0.003 \pm 0.031) \\ A_{\rm obs}^{>450\ \rm GeV} &= 0.212 \pm 0.096(\text{stat.}) \qquad (\text{Pred.} :\ -0.040 \pm 0.055)\ . \end{aligned}$$

IV. CORRECTIONS

Background contributions in the observed $\Delta y_{t-\bar{t}}$ and $\Delta\eta_\ell$ distributions are estimated using diboson, Drell-Yan Monte Carlo samples, and fake candidates. We check the background prediction using the control samples where these events pass the criteria of the event selection except that the number of jets is 0 or 1. Figure 10 shows the observed $\Delta\eta_\ell$ distributions and their prediction for 0 and 1 jet control samples. The $\Delta\eta_\ell$ distributions for the control samples are well predicted.

The asymmetries of $\Delta y_{t-\bar{t}}$ and $\Delta\eta_\ell$ distributions after subtracting the background contributions are estimated to be $A_{t-\bar{t}}(\text{bkg} - \text{sub}) = 0.21 \pm 0.07(\text{stat.}) \pm 0.02(\text{bkg. shape})$ and $A_{\rm sub}^{\Delta\eta_\ell} = 0.21 \pm 0.07(\text{stat.}) \pm 0.02(\text{bkg. shape})$, respectively. Here we consider systematics due to uncertainty in background shape and number estimation. Figure 11 shows the observed, expected background and background subtracted $\Delta y_{t-\bar{t}}$ distributions.

The asymmetry shown in the background subtracted $\Delta y_{t-\bar{t}}$ distribution is smaller than the true asymmetry. This is because that the acceptance is dependent on $\Delta y_{t-\bar{t}}$; also there is dilution due to the detector resolution and reconstruction.

We estimate the expected asymmetry of background subtracted $\Delta y_{t-\bar{t}}$ distribution as a function of true asymmetry using $t\bar{t}$ Monte Carlo. We adopt phenomenological asymmetry model on the Monte Carlo, i.e. the assumption of the asymmetry is approximately a linear function of $\Delta y_{t-\bar{t}}$. Based on the assumption, we correct the background subtracted asymmetry to obtain the true asymmetry of $\Delta y_{t-\bar{t}}$.

Our measured asymmetry of $\Delta y_{t-\bar{t}}$, after correction, is found to be $A_{\rm true} = 0.42 \pm 0.15(\text{stat.}) \pm 0.04(\text{bkg} - \text{shape})$.

V. SYSTEMATIC UNCERTAINTIES

A number of systematic effects contribute to our measurement uncertainty in a way that is not yet reflected in our calculation. Each systematic is estimated in a unique way, but the general procedure is to compare the measured result of a $t\bar{t}$ Monte Carlo model before and after a systematic has been varied. The Jet Energy Scale is estimated by fluctuating the model by the known uncertainties in JES by $\pm 1\sigma$. Samples of Monte Carlo were generated with more and less initial and final state radiation to estimate the impact of each. As described above, this measurement has been tested for a number of different underlying production angle distributions. The variance between different distributions has been taken as a systematic. The normalization of our background and the shape of the Monte Carlo model are varied within error and the difference in the measurement of our example models is taken as a systematic. Finally, we use 46 different sets of PDF and compare to the default set used. Table II summarizes the uncertainty taken for each systematic effect. The dominant uncertainty is due to background shape and normalizations, and top mass - though the top mass systematic is most likely due to limited statistics in that comparison. The combined systematic uncertainty on the measurement of A_{fb} is calculated by adding each individual uncertainty in quadrature. The result is shown in Table II. The largest systematic uncertainty comes from the shape of our backgrounds, particularly the data-derived shape of our fake lepton sample.

TABLE II: The summary of systematics sources and contributions to the total systematic uncertainty

Source	Systematics to A_{true}
Background Shape	0.04
Detector Modeling	0.01
Signal MC	0.02
ISR/FSR	0.02
Jet Energy Scale	0.01
Color Reconnection	0.01
PDF	<0.01
Total	0.05

VI. CONCLUSION

We have developed a method of reconstructing $t\bar{t}$ events in the dilepton channel and applied this to a measurement of the front-back asymmetry in top production in 5.1 pb^{-1} of proton-antiproton collisions at $\sqrt{s} = 1.96$ TeV. The measurement is a test of charge asymmetry in the strong interaction at large momentum transfer. In the present data set it is also potentially sensitive to large parity violating contributions to top production. The front-back asymmetry is measured to be:

$$A_{fb} = 0.42 \pm (0.15)^{stat} \pm (0.05)^{syst}$$

The measured asymmetry is 2.6 σ from zero, and 2.3 σ from the standard model prediction, 0.06.

Acknowledgments

We thank the Fermilab staff and the technical staffs of the participating institutions for their vital contributions. This work was supported by the U.S. Department of Energy and National Science Foundation; the Italian Istituto Nazionale di Fisica Nucleare; the Ministry of Education, Culture, Sports, Science and Technology of Japan; the Natural Sciences and Engineering Research Council of Canada; the National Science Council of the Republic of China; the Swiss National Science Foundation; the A.P. Sloan Foundation; the Bundesministerium für Bildung und Forschung, Germany; the Korean Science and Engineering Foundation and the Korean Research Foundation; the Science and Technology Facilities Council and the Royal Society, UK; the Institut National de Physique Nucleaire et Physique des Particules/CNRS; the Russian Foundation for Basic Research; the Comisión Interministerial de Ciencia

y Tecnología, Spain; the European Community's Human Potential Programme; the Slovak R&D Agency; and the Academy of Finland.

---

[1] cdf2now (CDF Collaboration), arXiv:hep-ex/1101.0034 (2011).
[2] J. Kuhn and G. Rodrigo, arXiv:hep-ph/0701166 (2007).
[3] T. Aaltonen et al. (CDF Collaboration), Phys. Rev. Lett. **105**, 012001 (2010).
[4] D. Acosta et al. (CDF Collaboration), Phys. Rev. D **71**, 032001 (2005).
[5] A. Abulencia et al. (CDF Collaboration), J.Phys. G Nucl.Part.Phys. **34**, 2457 (2007).
[6] S. Moch and P. Uwer, Nucl. Phys. Proc. Suppl. **183**, 75 (2008).
[7] CDF uses a cylindrical coordinate system with the z axis along the proton beam axis. Pseudorapidity is $\eta \equiv -\ln(\tan(\theta/2))$, where θ is the polar angle, and ϕ is the azimuthal angle relative to the proton beam direction, while $p_T = |p| \ \sin(\theta)$, $E_T = E \ \sin(\theta)$.
[8] Missing transverse energy, $\not\!\!E_T$, is defined as the magnitude of the vector $-\sum_i E_T^i \vec{n}_i$ where E_T^i are the magnitudes of transverse energy contained in each calorimeter tower i, and $\vec{n}_i$ is the unit vector from the interaction vertex to the tower in the transverse (x, y) plane.
[9] A. Bhatti et al., Nucl. Instrum. Methods **A566**, 375 (2006).
[10] M. L. Mangano et al., J. High Energy Phys. **001**, 0307 (2003).
[11] M. L. Mangano et al., Nucl. Phys. B **632**, 343 (2002).
[12] F. Caravaglios et al., Nucl. Phys. B **539**, 215 (1999).
[13] T. Sjostrand et al., Comp. Phys. Commun. **135**, 238 (2001).
[14] J. Alwall et al., J. High Energy Phys. **28**, 709 (2007).
[15] P. Nadolsky et al. (CTEQ Collaboration), Phys. Rev. D **78**, 013004 (2008).
[16] E. Gerchtein and M. Paulini, arXiv:physics/0306031 (2003).
[17] S. Agostinelli et al., Nucl. Instrum. Methods **A506**, 250 (2003).
[18] T. Aaltonen et al. (CDF Collaboration), CDF Public Note **10163** (2010).

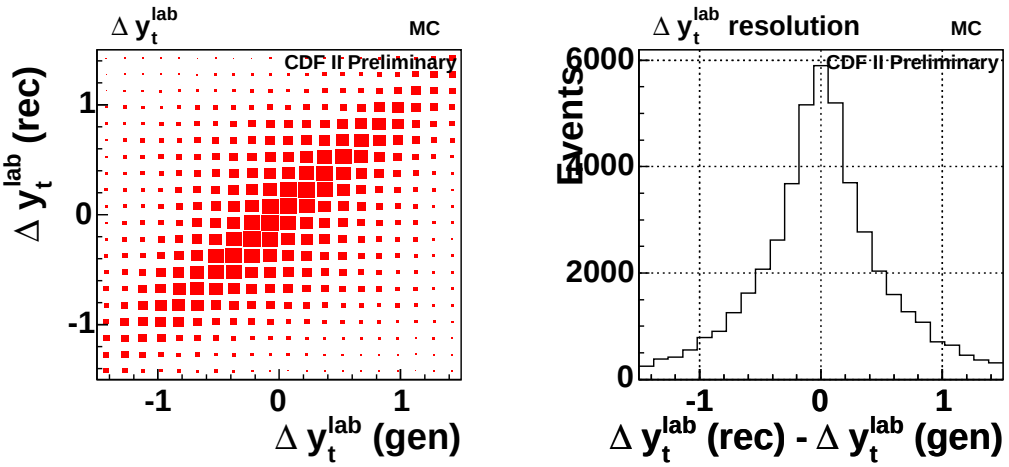

FIG. 1: The forward backward asymmetry of the production of top quarks is calculated from the difference in rapidity between the reconstructed top and anti-top quarks. This figure demonstrates the performance of the reconstruction algorithm to calculate the rapidity difference.

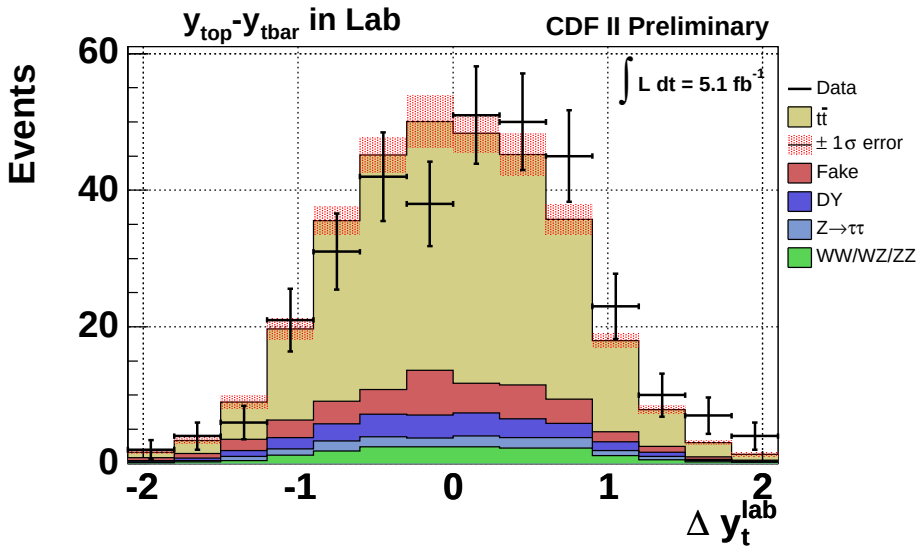

FIG. 2: The rapidity between the reconstructed top and anti-top quarks in data and in the predicted signal and background simulations. The reconstructed forward backward asymmetry in data is $A_{fb} = 0.14 \pm 0.05$.

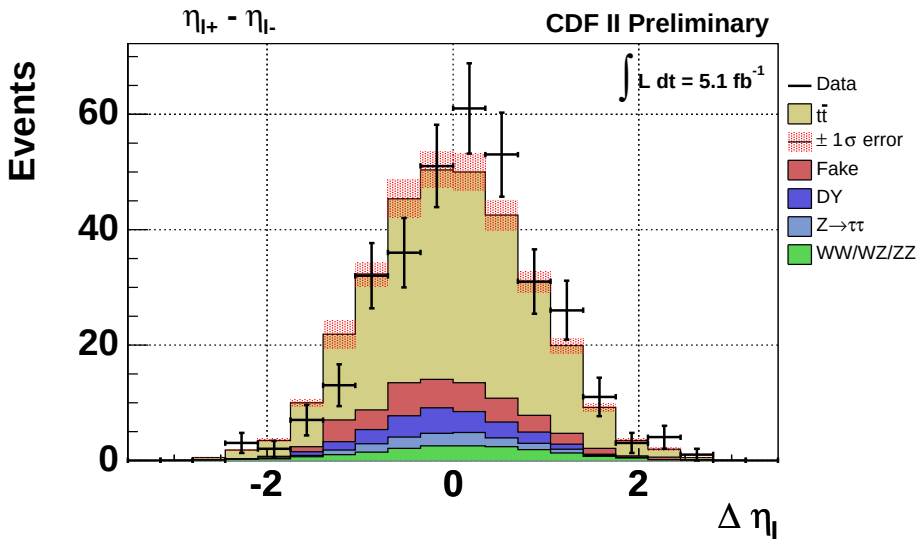

FIG. 3: The rapidity between the positively and negatively charged leptons in data and in the predicted signal and background simulations. The forward backward asymmetry in data is $A_{fb} = 0.14 \pm 0.05$.

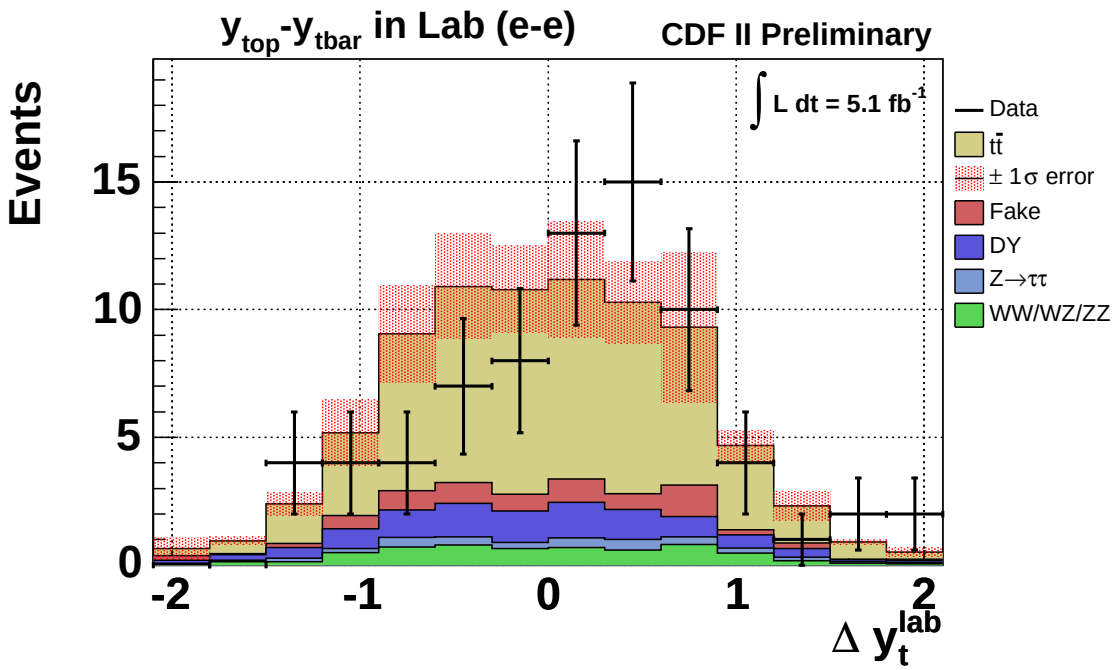

FIG. 4: $A^{ee}_{\rm obs} = 0.270 \pm 0.112$(stat.) (Pred.: -0.010 ± 0.070). K-S probability is calculated to be 2.5 %.

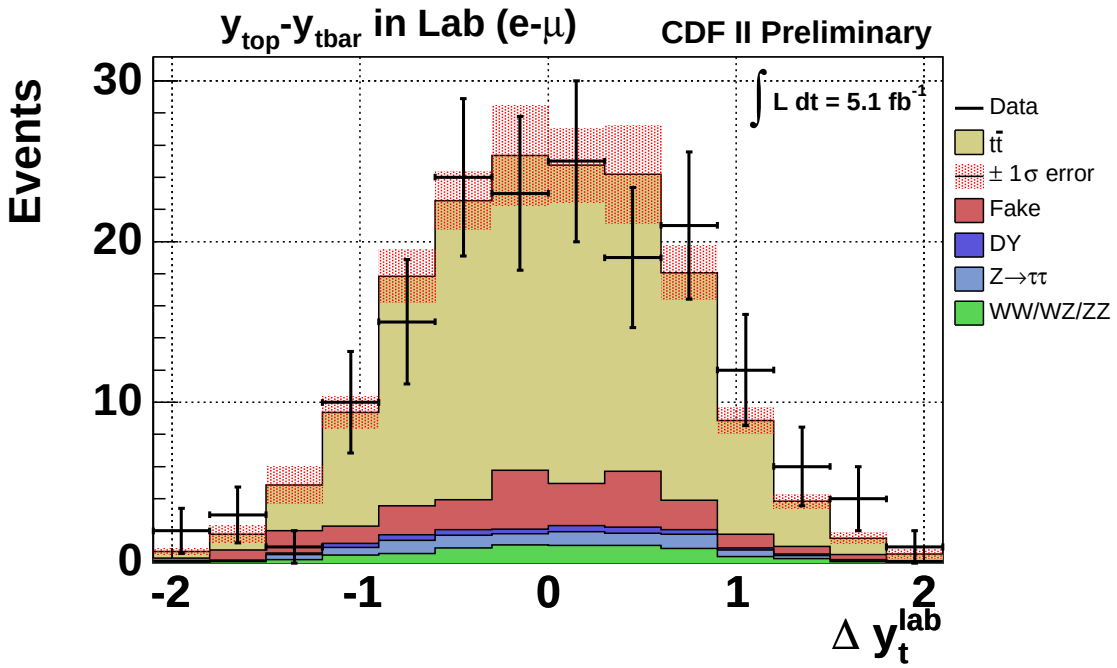

FIG. 5: $A^{e\mu}_{\rm obs} = 0.060 \pm 0.077$(stat.) (Pred.: -0.004 ± 0.037). K-S probability is calculated to be 21.7 %.

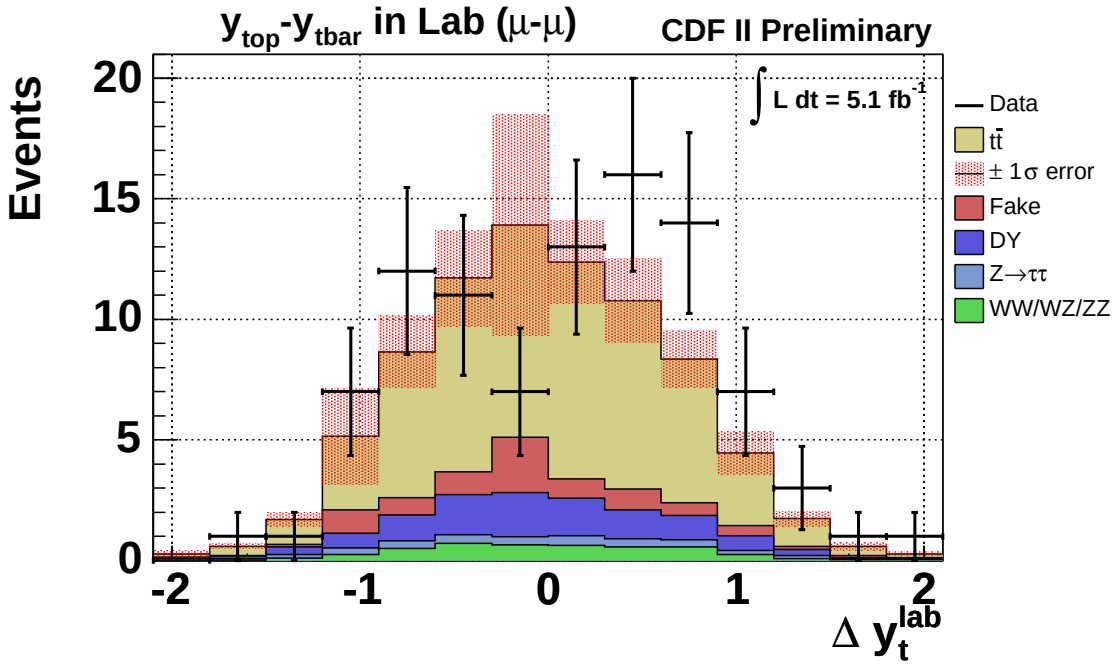

FIG. 6: $A^{\mu\mu}_{\rm obs} = 0.170 \pm 0.102$(stat.) (Pred.: -0.039 ± 0.078). K-S probability is calculated to be 8.0 %.

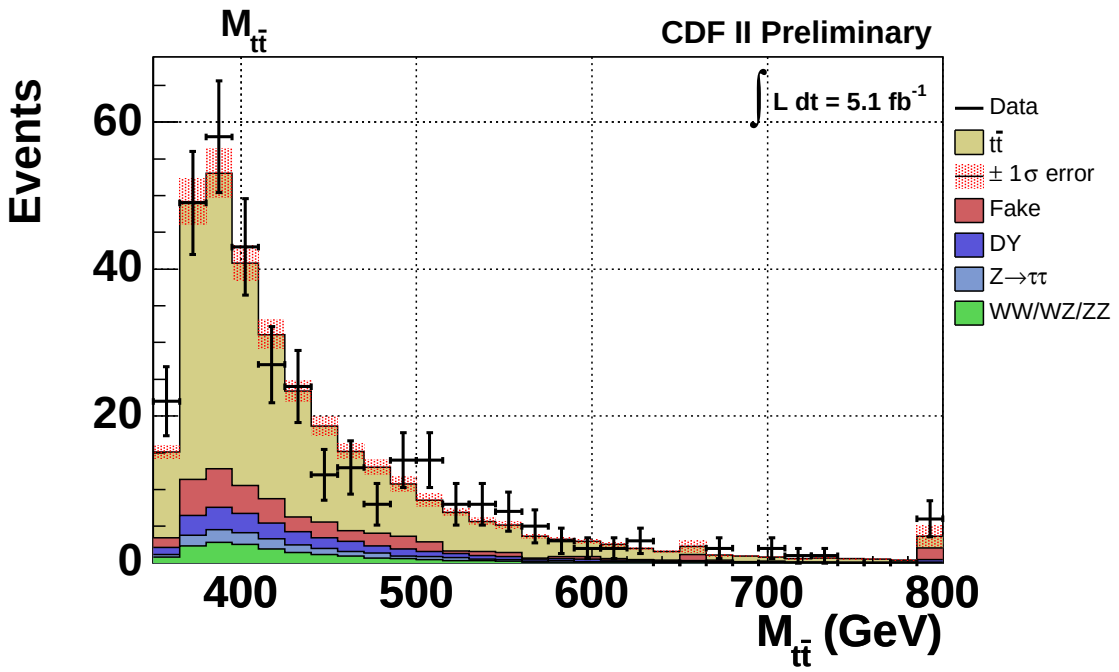

FIG. 7: The reconstructed $M_{t\bar{t}}$ distribution of dilepton candidates in 5.1 fb^{-1} data. The crosses indicate data, and histogram and the hatched band show expected signal and background events with $\pm 1\sigma$ uncertainty. K-S probability is found to be 60.5 %.

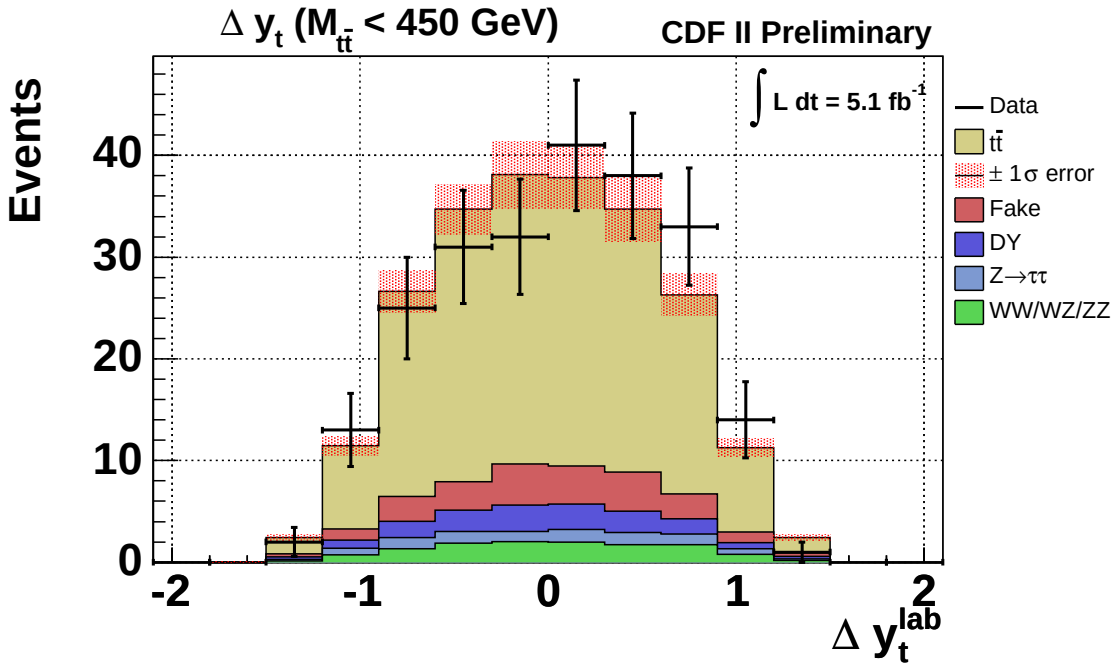

FIG. 8: The reconstructed Δy_t distribution of the 230 dilepton candidates out of 334 total candidates where the reconstructed $M_{t\bar{t}} < 450$ GeV is required. We find 127 events in the positive side, while 103 in the negative side. The raw asymmetry is calculated to be $A_{\rm obs}^{<450\ \rm GeV} = 0.104 \pm 0.066(\rm stat.)$ (Pred. : -0.003 ± 0.031).

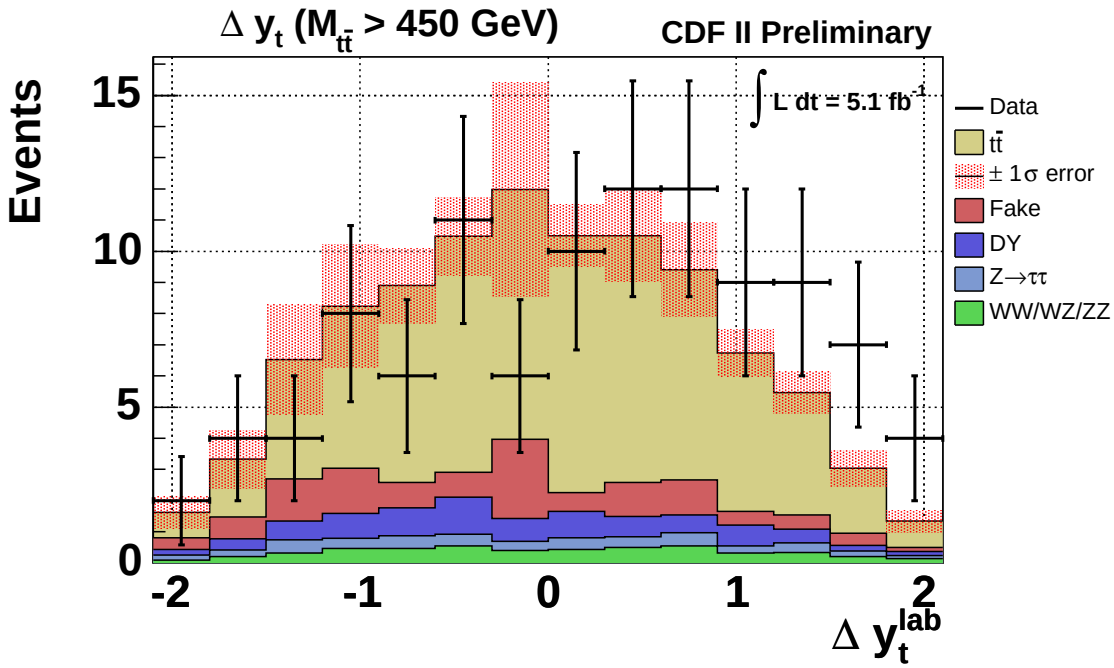

FIG. 9: The reconstructed Δy_t distribution of the 104 dilepton candidates out of 334 total candidates where the reconstructed $M_{t\bar{t}} > 450$ GeV is required. We find 63 events in the positive side, while 41 in the negative side. The raw asymmetry is calculated to be $A_{\rm obs}^{>450\ {\rm GeV}} = 0.212 \pm 0.096({\rm stat.})$ (Pred. : -0.040 ± 0.055).

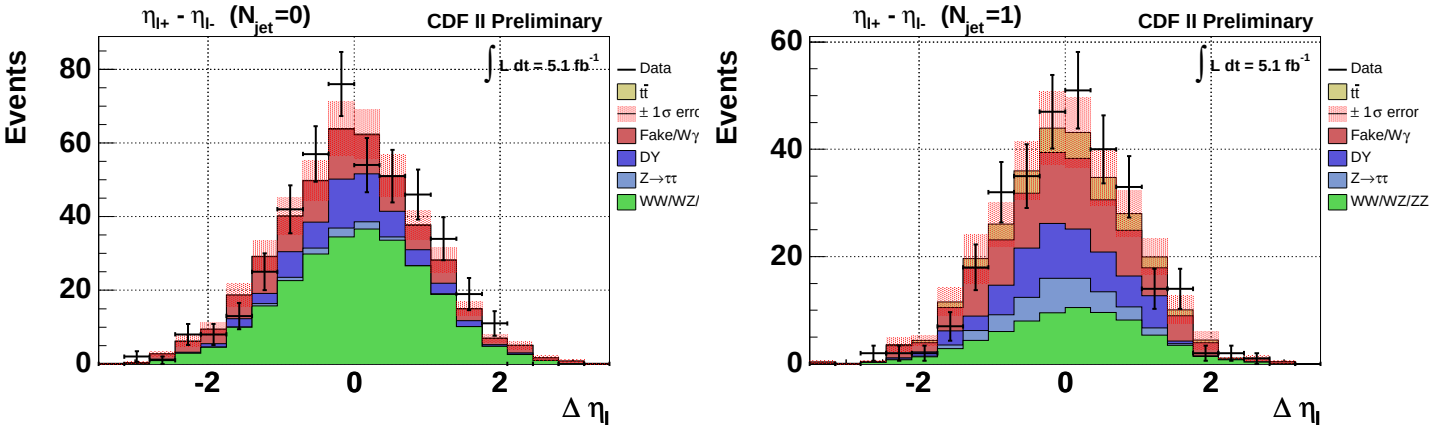

FIG. 10: The reconstructed $\Delta\eta_\ell$ distribution of the dilepton candidates in the data, but the number of jets is 0 (left) and 1 (right). H_T cut is not applied.

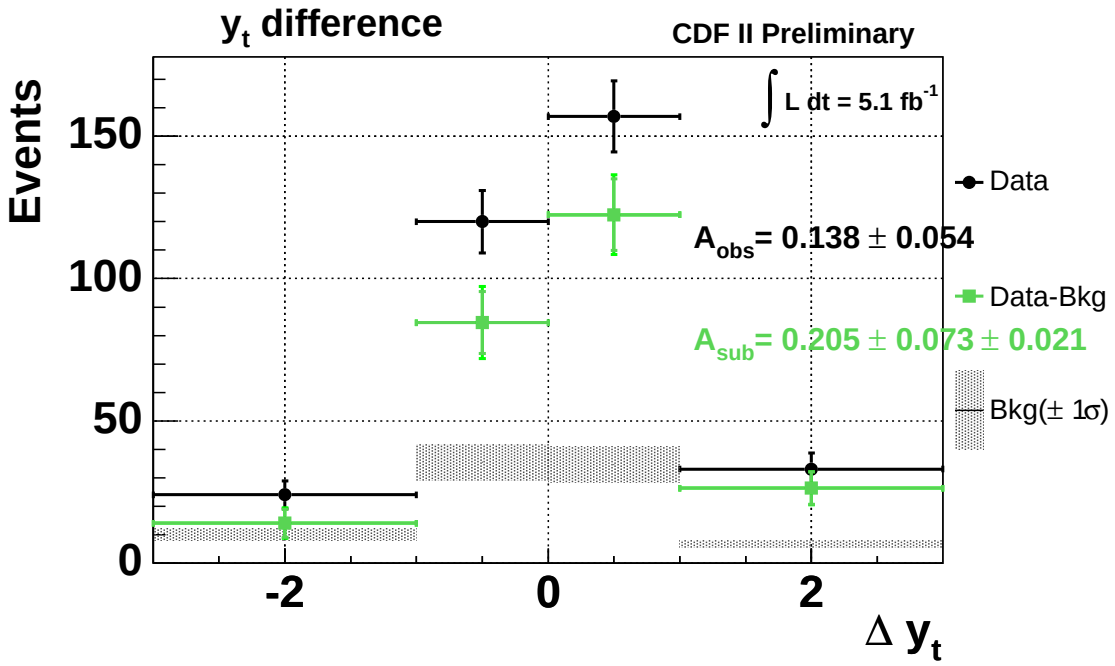

FIG. 11: The observed (black), expected background (gray band) and background subtracted (green) $\Delta y_{t-\bar{t}}$ distributions.